Research Article

Analysis of the Effect of Switching Frequency on Acoustic Noise in External Rotor Brushless DC Motors

Bugra Er, Berk Demirsoy, Ahmet Fenercioglu

***Abstract*— Electric motors are widely used in various industries and are subject to specific acoustic noise standards depending on their applications. Despite their superior performance compared to brushed motors, brushless motors generate acoustic noise due to their mechanical, electrical, and electronic components. This study investigates the effect of changing the switching frequency through the driver on the acoustic noise of an external rotor brushless DC motor. Tests were conducted on a surface-mounted magnetic brushless motor with different switching frequencies, and detailed information about the control board governing the brushless motor was provided. Sound intensity and harmonic measurements were conducted with a dB meter in an anechoic quiet room. Changing the switching frequency also affects the motor speed, so two different measurements were taken during the study. In one test, the BLDC motor speed was kept constant, while in the other, the Duty cycle ratio was kept constant for measurements. An increase in the switching frequency was observed to reduce motor noise. However, this increase also leads to losses in the switching components, resulting in a temperature increase. The speed of the external rotor brushless DC motor was kept constant by adjusting the Duty cycle while changing the switching frequency. Increasing the switching frequency in the range of 12-28 kHz reduced the measured acoustic noise while causing temperature increases in different frequency ranges. The study's results indicate that the existing BLDC motor and driver system provide optimum performance in terms of acoustic noise and temperature in the 16-18 kHz range.**

Index Terms— **Acoustic noise, BLDC motor, Switching frequencies.**

I. Introduction

BLDC(Brushless Direct Current) motor has a high starting torque and is often preferred in variable-speed applications. It can minimize mechanical wear, noise, and temperature without brushes [1]. Due to the absence of brush friction, it emits lower acoustic noise.

The control algorithm for BLDC motors is considerably complex compared to brushed DC motors [2]. The rotor position needs to be detected and commutation must be performed. Hall-effect sensors are used for rotor position sensing [3]. By evaluating the data from three sensors, the BLDC motor triggers the appropriate phase for operation. Control of switching angles is essential, especially during acceleration. The signal applied to the switching elements contains PWM (Pulse Width Modulation) signals. The switching frequency of this PWM signal is of great importance. Parameters related to the time constant are directly related to the switching frequency and rotor frequency [4].

BLDC motor is classified into two categories based on its mechanical structures: bearing, housing, rotor, and stator assembly, and BLDC motor control approaches [5]. While BLDC motor parameters remain constant during system operation, practical applications involve continuously changing parameters such as mechanical load and friction [6]. Factors like friction among these mechanical elements can contribute to mechanical noise [7]. Additionally, conditions such as the influence of bearing, shaft vibration, and rotor eccentricity can also generate noise [8]. In this context, mechanical factors and noise are significant considerations in BLDC motor systems. The electrical noise sources in the BLDC motor system are illustrated in Figure 1 [9].

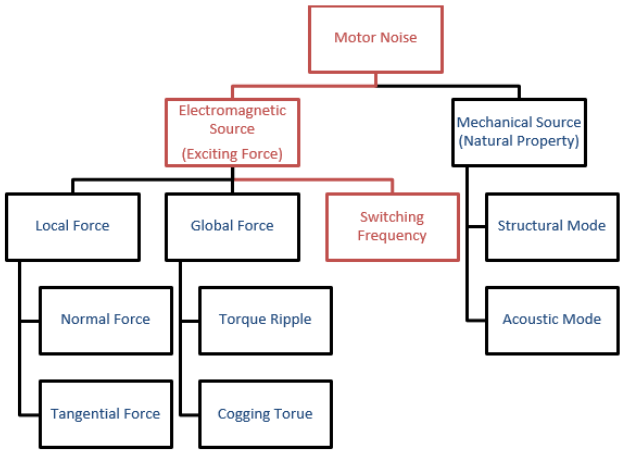

Fig 1. BLDC motor noise

Buğra Er, is Kormas Elektrikli Motor A.Ş. TOSB OSB, Kocaeli, Turkey, (e-mail: bugraer@kormas.com).
https://orcid.org/0000-0002-3982-5654
Berk Demirsoy, is Kormas Elektrikli Motor A.Ş. TOSB OSB, Kocaeli, Turkey, (e-mail: berkdemirsoy@kormas.com).
https://orcid.org/0009-0003-3489-7346
Ahmet Fenercioğlu, is Department of Mechatronic Engineering, Bursa Technical University, 16310, Bursa Turkey, (e-mail: ahmet.fenercioglu@btu.edu.tr).
https://orcid.org/0000-0002-1522-6868
Manuscript received July 5, 2023; accepted Oct 03, 2023.
DOI: 10.17694/bajece.1322919

These sources include factors such as motor power and switching frequency, which contribute to motor noise. Additionally, the motor mechanics, depending on the mechanical design, can directly influence the sound. Electromagnetic sources can also impact the noise level in BLDC motor design [10]. Holding torque and torque fluctuations are other factors that affect the sound and are examined as a separate field. Acoustic noise refers to unwanted audible sound and is of significant importance as it emanates from a vibrating object. Current variation and the fundamental frequency of acoustic noise originating from the current cause electromagnetic noise in the BLDC motor's commutation frequency [11]. In this study, the designed board in Altium Designer software includes ST Microelectronics components, an IPM (Intelligent Power Module), and an STM32G030 microcontroller. Real-time drive parameters can be analyzed and manipulated through Keil u5. By gradually changing the switching frequency from 12kHz to 28kHz, the motor speed, motor sound, motor current, and motor phase signals were examined.

II. External Rotor BLDC Motor and Driver Design

Acoustic noise in a system containing a motor is influenced by electromagnetic, mechanical, aerodynamic, and electrical sources [12]. Electromagnetic noise and vibration on the motor can be affected by factors such as stator shape and slot opening, phase imbalances, high airgap harmonics, and the magnetic saturation of the used core. Mechanical noise and vibration are influenced by the motor's assembly, while aerodynamic noise and vibration can be related to airflow in the motor's ventilation channels [13-14]. Additionally, reducing electromagnetic noise in BLDC motors relies on reducing torque ripple [15]. Various factors can contribute to torque ripple in electric motors, including cogging torque, non-ideal back-EMF (Electromotive Force) waveform, PWM current harmonics, and phase commutation. At high speeds, the system's inertia can compensate for torque ripple, but at low speeds, torque ripple can cause unacceptable levels of vibration and acoustic noise [16]. To reduce acoustic noise related to torque ripple, studies have been conducted on the number of poles and cogging torque in BLDC motor designs. Cogging torque can hinder the smooth operation and desired speed of the motor, leading to acoustic noise. The number of poles in the BLDC motor design has an impact on its acoustic noise [17]. Table 1 below provides the system parameters of the BLDC motor and the driver.

Table I
SYSTEM PARAMETERS OF THE MOTOR AND DRİVER

Motor	Input Voltage	310 V_{DC}
	Number of Poles/Slots	18/20
	Phase resistance	3.2 Ω
	Phase inductance	10.42mH
Driver	Inverter Type	Six-Step Driver
	Control Signal	PWM
	Switching Frequency	Variable frequency

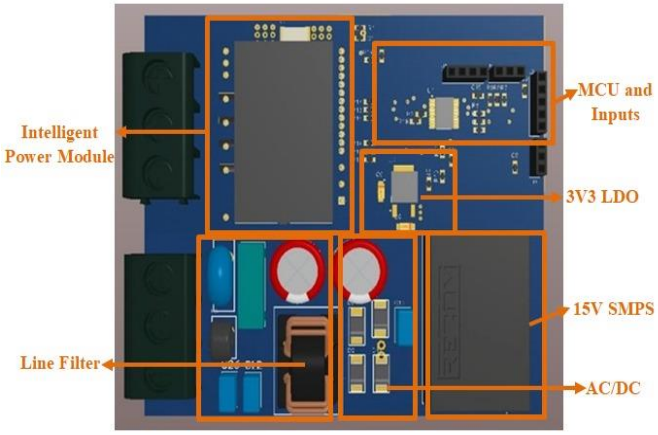

Fig 2. BLDC motor driver

The BLDC motor driver is a necessary component in the control of BLDC motor systems. In this study, an IPM is used as the power stage. The IPM has a rating of 600V and 15A, and it includes the necessary pins for the IGBT driver, IGBT, and bootstrap structure. The switching elements represented by the symbol 'S' in the design are implemented as IGBTs. The power supply of the system is determined as $220V_{AC}$, and AC-DC conversion is performed using bridge diodes. Then, a switched-mode power supply is used to obtain 15V. A 3V regulator is available for the STM32 microcontroller and the Hall-effect sensors used in the STM32 series. The 3V regulator and IGBT drivers are powered by the 15V power supply. The control circuit consists of the microcontroller and the system inputs. The driver circuit is responsible for distributing the energy from the source to the motor phases according to the signals from the control circuit. The relevant components are shown in Figure 2 on a PCB design using Altium Designer. The structure of the motor driver sections provided in Figure 2 is detailed in Figure 3 and Figure 4.

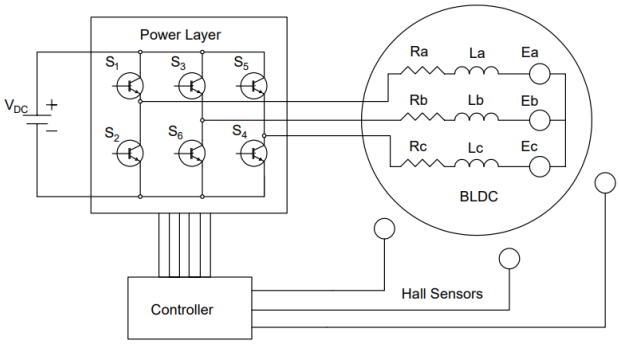

Fig 3. Driver diagram

The diagram provided in Figure 3 depicts the use of Hall sensors to detect the rotor position, which is then communicated to the controller to transmit the necessary signals to the power layer [18]. By transmitting 6 PWM signals, the control of three half-bridge structures is achieved. Each half-bridge structure controls one phase of the motor. The diagram represents a three-phase motor configuration. The back-EMF of each phase has a trapezoidal waveform [19]. The trapezoidal signals between phases have a phase difference of 120 electrical degrees [20].

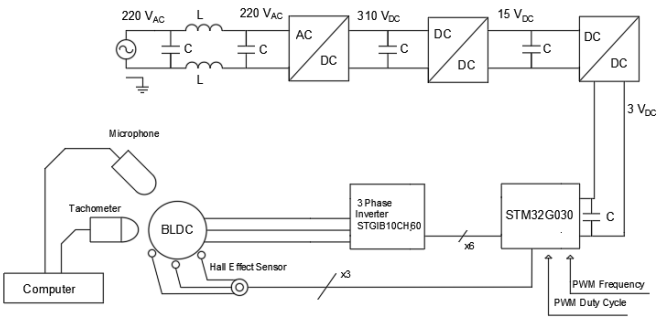

Fig 4. Schematic diagram of the experimental setup

III. Acoustic Model and Testing

Figure 4 illustrates the schematic diagram of the test system. The system operates with a 220V AC input, which is then converted to DC 310V through a line filter and rectifier supply. The control layer obtains 15V and 3V DC voltages, which are utilized for powering the controller and hall sensors. Based on the rotor position detected by the hall sensors, control signals are transmitted to the power layer for BLDC motor control through 310V DC switching. A tachometer is employed in the system to measure the BLDC motor speed. By varying the switching frequency and duty cycle, sound measurements are performed and recorded via the BLDC motor driver and BLDC motor system.

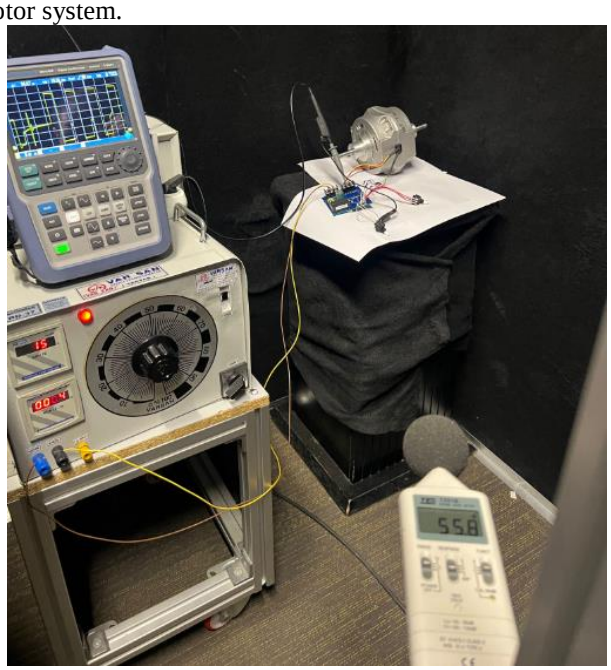

Fig 5. Acoustic noise test environment of BLDC motor system

To investigate the acoustic noise characteristics, measurements are conducted at different motor speeds using the test setup shown in Figure 5. For noise measurement, a vertical sound level meter is placed 1 meter away from the motor. The motor speed is obtained using a BLDC motor tachometer. The options for frequency response include A and C weighting. We conducted the measurements using the A-weighting frequency response, which is closer to the sensitivity of the human ear. The experiment was performed with a sound level meter that has a sensitivity of 0.1 dB. The measurement system comprises a sound level meter, a BLDC motor, an AC power supply, and a computer. The utilized sound level meter complies with the IEC 60804-2000 Type 1 standard and has a measurement error of less than 0.5 dB. The microphone used for noise measurement is vertically positioned at a distance of 1 meter from the motor [10]. The same 1-meter measurement distance has also been applied in motor studies conducted in the HVAC field. Acoustic noise was measured in accordance with ISO 3741 standard at four different points horizontally, 1 meter away from the BLDC motor.

The tests were conducted in a 10m² anechoic room, where the motor was not operational but the power sources connected to the motor were active. Anechoic materials and sound insulators were used to ensure sound isolation. In the absence of motor operation, a sound measurement of 36 dB was obtained from the system. Rohde & Schwarz oscilloscope and interfaces were utilized for controlling the system's key frequency and phase diagrams. Variac was used as the power source in the system for voltage and current monitoring. It has no visible effect on the phase plots. During the BLDC motor testing, the waveform at a 50% duty cycle and a switching frequency of 20 kHz with a peak value of 310 Vdc is shown in Figure 6. Figure 7 represents a representation of the switching frequency within the phase signal.

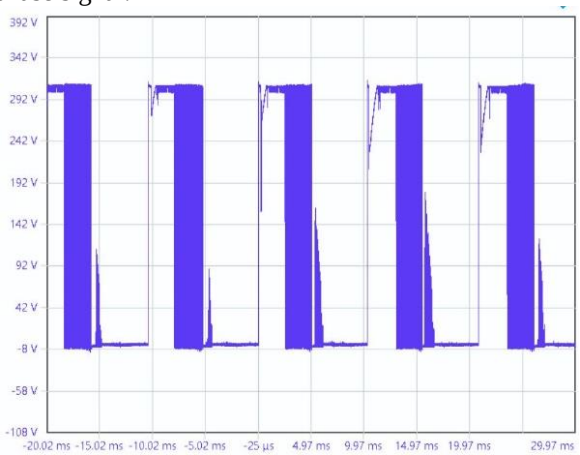

Fig 6. BLDC motor phase signal (%50 PWM 20kHz)

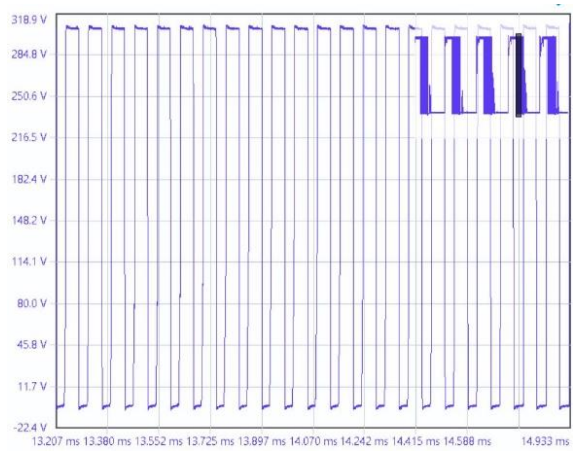

Fig 7. Extended version of BLDC motor signal

The motor was operated at switching frequencies ranging from 12 kHz to 28 kHz during the experiments. During the tests, the

applied PWM values to the BLDC motor, system voltage, noise level, current consumption of the system, and BLDC motor speed were measured. Additionally, the motor frequency corresponding to the speed was obtained.

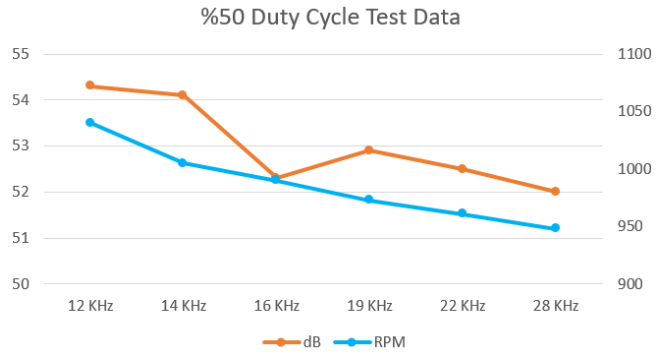

Fig 8. Noise graph with %50 Duty Cycle BLDC motor variable switching frequency and RPM

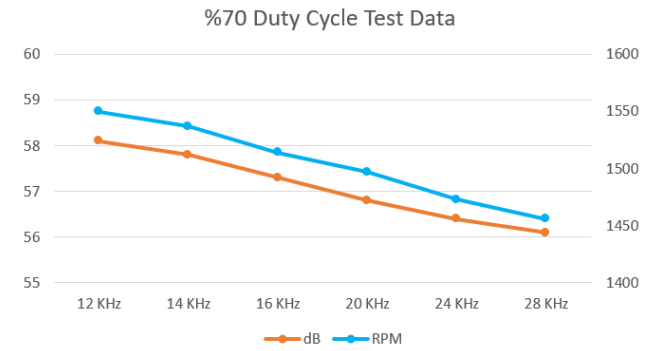

Fig 9. Noise graph with %70 duty cycle BLDC Motor variable switching frequency and RPM

In the graphs obtained in Figure 8 and Figure 9, the variation in motor RPM(Revolutions per Minute) is observed as the switching frequency is changed. During the tests, measurements were taken as the switching frequency increased, and the decrease in motor speed was plotted on the graph as the noise level in dB. As the frequency increases, the motor speed decreases, leading to a reduction in mechanical noise. The graphs obtained in Figures 10 and 11 show the change in acoustic noise as the switching frequency changes while keeping the motor speed constant.

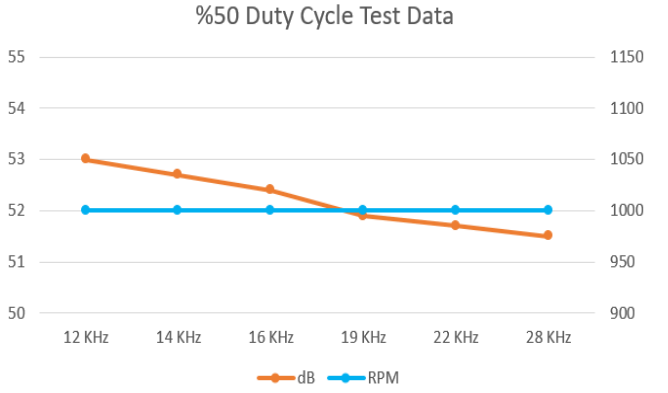

Fig 10. Noise graph with BLDC Motor variable switching frequency and duty cycle, constant 1000RPM

On the horizontal axis, the switching signals ranging from 12kHz to 28kHz are applied to the motor drive, and the resulting noise levels in dB are given on the vertical axis. The increase in motor speed contributes to an increase in the mechanically generated sound level. In tests conducted with different duty cycle values, the minimum amount of acoustic noise varies. In Figure 11 and Figure 12, the acoustic noise graph is presented for variable switching frequencies while maintaining a constant speed.

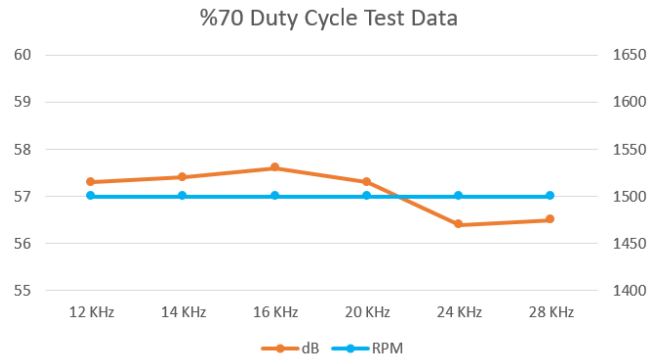

Fig 11. Noise graph with BLDC Motor variable switching frequency and duty cycle, constant 1500 RPM

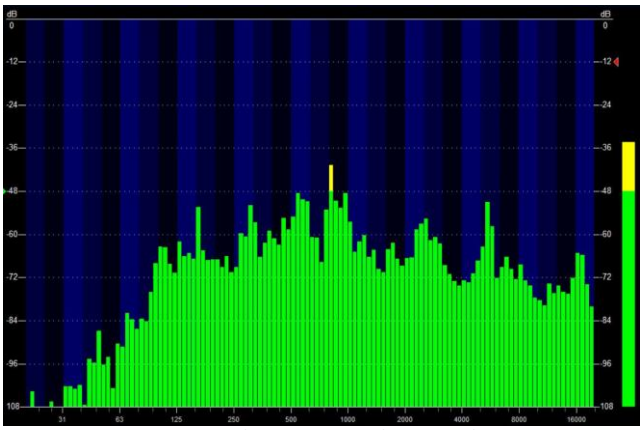

Fig 12. Display of acoustic noise frequency for 28khz

Figures 12, 13, 14, and 15 provide data on acoustic noise frequencies. These graphs illustrate how reducing the switching frequency affects the frequency of acoustic noise. The horizontal axis represents the frequency of acoustic noise, while the vertical axis indicates the sound intensity in dB. For example, in Figure 12, when the switching frequency is 16 kHz, it is observed that the levels of acoustic noise drop to as low as 8 kHz in Figure 15. These findings indicate that as the switching frequency decreases, acoustic noise approaches a range perceptible to the human ear, considering the audible frequency range. However, increasing the switching frequency, while potentially shifting acoustic noise to frequencies beyond the human ear's perception, necessitates considering the electrical stress and temperature values on components when making such a decision.

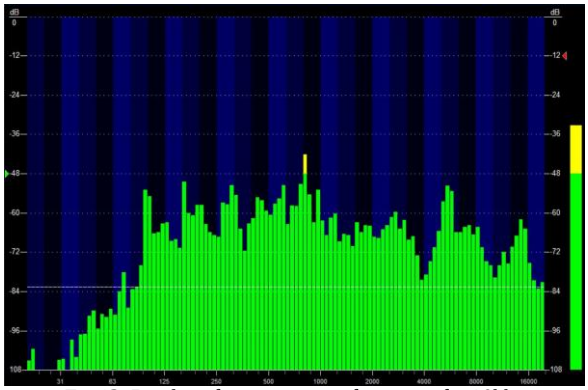

Fig 13. Display of acoustic noise frequency for 20khz

Fig 14. Display of acoustic noise frequency for 16khz

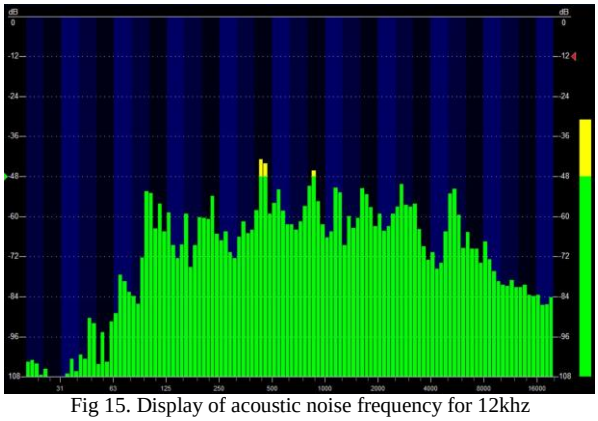

Fig 15. Display of acoustic noise frequency for 12khz

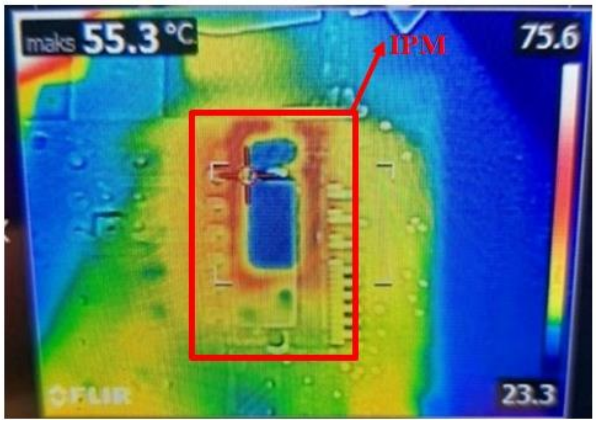

Fig 16. IPM temperature graph at tested switching

TABLE II
SYSTEM PARAMETERS

	12kHz	14kHz	16kHz	19kHz	22kHz	28kHz
Step Times (sec)	200	200	200	200	200	200
Output Power (W)	55.9	55.9	55.9	55.9	55.9	55.9
Output Frequency (Hz)	166	166	166	166	166	166
Transmission and Switching Loss (W)	0.28	0.31	0.34	0.39	0.44	0.50
Total Loss (W)	0.28	0.31	0.34	0.39	0.43	0.50
Junction Temperature (°C)	57.80	61.30	64.90	70.54	76.44	84.86

The switching frequency has a significant impact on the motor speed. Additionally, the operating sound of the motor is directly related to the switching frequency. Figure 16 presents the temperature map of the IPM (Intelligent Power Module) for a switching frequency of 12kHz. The losses occur in the switching elements due to their internal resistances and switching losses. These losses directly affect the temperature of the IPM. Various simulation programs are available for component manufacturers to simulate power modules or products. ST Microelectronics provides the STpowerStudio program specifically for IPM modules. Table 2 provides input data for switching frequencies, motor frequencies, and input voltage, along with their respective durations. Each case was subjected to a 200-second simulation, during which no significant temperature changes were observed. Subsequently, temperature data was obtained using these inputs and calculated for the STGIB10CH60S IPM product using the program, resulting in the generation of graphs. These graphs are presented in Figure 17. The results obtained from the tests highlight the importance of correctly selecting the switching frequency.

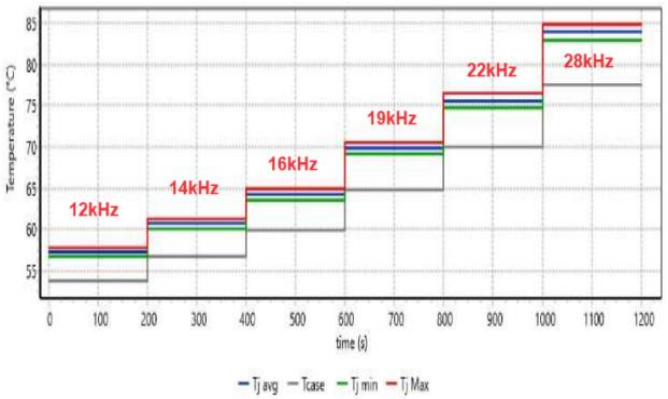

Fig 17. IPM at switching frequency changes

VI. CONCLUSIONS

This research focuses on examining the impact of frequency variations on the efficiency, cost, and reliability of BLDC motors. Speed control was achieved by applying PWM signals to switching elements based on rotor position information. Frequency changes were measured using a scale recorder powered by an STM32F031 Microcontroller. The experiments revealed that lower frequencies yielded better results under high load conditions. In balanced load conditions, determining the optimal frequency is a priority. Oscilloscope data, presented with various graphs ranging from 12 kHz to 28 kHz, clearly illustrate the variation of the switching frequency in phase-neutral graphs. Data collected from motor experiments are also shared. Sound intensity and harmonic measurements were conducted with a dB meter in an anechoic quiet room. Changing the switching frequency also affects the motor speed; hence, two different measurements were conducted during the study. In one test, the BLDC motor speed was kept constant, while in the other, the Duty cycle ratio was maintained at a constant level for measurements. An increase in the switching frequency is shown to reduce motor noise. However, this increase also leads to increased losses in the switching components, resulting in a temperature rise. The speed of the external rotor brushless DC motor was kept constant by adjusting the Duty cycle while changing the switching frequency. Increasing the switching frequency in the range of 12-28 kHz reduced motor speed while decreasing the measured acoustic noise. However, temperature increases were observed in different frequency ranges. The study's results demonstrate that the existing BLDC motor and driver system provide optimum performance in terms of acoustic noise and temperature in the 16-18 kHz range. These findings can serve as a valuable source of information for industry professionals looking to optimize the performance of BLDC motors.

REFERENCES

[1] M.R. Hazari, E. Jahan, M.E. Siraj, M.T.I. Khan, A.M. Saleque. “Design of a Brushless DC (BLDC) motor controller.” In 2014 International Conference on Electrical Engineering and Information & Communication Technology. IEEE, 2014, pp 1-6.

[2] P. Yedamale. “Brushless DC (BLDC) motor fundamentals.” Microchip Technology Inc, vol. 20.1, 2003, pp 3-15.

[3] R.M. Pindoriya, A.K. Mishra, B.S. Rajpurohit, R. Kumar. “An analysis of vibration and acoustic noise of BLDC motor drive.” In 2018 IEEE Power & Energy Society General Meeting (PESGM), 2018, pp 1-5.

[4] P. Mishra, A. Banerjee, M. Ghosh, S. Gogoi, P.K. Meher. “Implementation and validation of quadral-duty digital PWM to develop a cost-optimized ASIC for BLDC motor drive.” Control Engineering Practice, vol. 109, 104752, 2021.

[5] K. Nakata, M. Sanada, S. Morimoto, Y. Takeda. “Noise reduction for switched reluctance motor with a hole.” Proceeding Power Converters Conference, vol. 3, 2002, pp 971-976.

[6] E. Serdar, Izci D., Yilmaz M. "Efficient speed control for DC motors using novel Gazelle simplex optimizer." IEEE Access, 2023, pp. 105830 – 105842.

[7] X.T. Bai, Y.H. Wu, K. Zhang, et al. “Radiation noise of the bearing applied to the ceramic motorized spindle based on the sub-source decomposition method.” J. Sound Vib., 410, 2017, pp 35-48.

[8] D.J. Kim, H.J. Kim, J.P. Hong, et al. “Estimation of acoustic noise and vibration in an induction machine considering rotor eccentricity.” IEEE Trans. Magn, vol. 50, 2, 2014, pp 857-860.

[9] H.J. Lee, S.U. Chung, S.M. Hwang. “Noise source identification of a BLDC motor.” Journal of mechanical science and Technology, vol. 22, 2008, pp 708-713.

[10] A. Lelkes, J. Krotsch, R.W. De Doncker. “Low-noise external rotor BLDC motor for fan applications in Conference Record of the 2002 IEEE Industry Applications Conference.” IEEE, vol. 3, 2002, pp 2036-2042.

[11] A. Sathyan, N. Milivojevic, Y.J. Lee, M. Krishnamurthy, A. Emadi. “An FPGA-based novel digital PWM control scheme for BLDC motor drives.” IEEE Transactions on Industrial Electronics, vol. 56. 8, 2009, pp 3040-3049.

[12] D.H. Cho, K.J. Kim. “Modeling of electromagnetic excitation forces of an induction motor for vibration and noise analysis.” Proceeding of the KSME Autumn A, 18 (2), 1997, pp 372-377.

[13] S. Nau, H. Mello. “Acoustic noise in induction motors: causes and solutions.” IEEE 2000 Petroleum and Chemical Industry Technical Conference, 2000, pp 253-263.

[14] B. Weilharter. “Noise Computation of Induction Machines.” 2012.

[15] S. Zuo, F. Lin, X. Wu. “Noise analysis, calculation, and reduction of external rotor permanent-magnet synchronous motor.” IEEE Trans. Ind. Electron., vol. 62.10, 2015, pp 6204-6212.

[16] T.M. Jahns, W.L. Soong. “Pulsating torque minimization techniques for permanent magnet AC motor drives-a review.” IEEE Transactions on industrial electronics, vol. 43. 2, 1996, pp 321-330.

[17] K.S. Kim, C.M. Lee, G.Y. Hwang, et al. “Effects of the number of poles on the acoustic noise from BLDC motors.” Springer J. Mech. Sci. Technol., vol. 25. 2, 2011, pp 273-277.

[18] A. Glowacz. “Thermographic fault diagnosis of ventilation in BLDC motors.” Sensors, 21(21), 2021, 7245.

[19] K.T. Chau, C.C. Chan, C. Liu. “Overview of permanent magnet brushless drives for electric and hybrid electric vehicles.” IEEE Transactions on Industrial Electronics, vol. 55, 6, 2008, pp 2246-2257.

[20] P.C. Desai, A. Emadi. “A novel digital control technique for brushless DC motor drives Current control.” IEEE Electronics Machine Drives Conference, 2005, pp 326-331.

BIOGRAPHIES

Buğra ER received the B.Sc. and M.Sc. degrees from Suleyman Demirel University, department of electrical education, Isparta, Turkey in 2020, 2023 respectively. He is currently a R&D engineer of Kormas Electric in Kocaeli, Turkey. His main research interests include electrical motor driver design and CANbus, HVAC control design, PCB design, permanent magnet synchronous motors and Brushless DC motors driver, power electronics for automotive applications.

Berk Demirsoy received his B.Sc. education in the Department of Electrical and Electronics Engineering at Sakarya University in 2021, and he is currently pursuing his M.Sc. in the Department of Electrical and Electronics Engineering at Sakarya Applied Sciences University. Sakarya, Turkey. He is currently a R&D engineer of Kormas Electric in Kocaeli, Turkey. His main research interests include electrical motor design and verification with FEM analyses, permanent magnet

synchronous motors, Brushless DC motors, induction motors, switched reluctance motors and power electronics applications.

Ahmet Fenercioğlu received the B.Sc. and M.Sc. degrees from Marmara University, department of electrical education, İstanbul, Turkey in 1994, 1996 respectively and the Ph.D. degree from Gazi University, Ankara, Turkey, in 2006. He is currently a Professor of Mechatronics Engineering Department at Bursa Technical University in Bursa, Turkey. His main research interests include electrical motor design and verification with FEM analyses, permenant magnet synchronous motors, induction motors, switched reluctance motors, power electronics and eddy current applications.